Supplementary Data

Metal-Coordination-Driven Self-Assembly of 8-Hydroxyquinoline-Peptide into Hybrid Nanomaterials for In Vitro Multimodal Synergistic Anticancer Activity

Shengyao Wang,[a] Xin Tian,*[b] and Xinming Li*[a]

[a.] College of Chemistry, Chemical Engineering and Materials Science, Soochow University, Suzhou 215123, China.

[b.] State Key Laboratory of Radiation Medicine and Protection, School for Radiological and Interdisciplinary Sciences (RAD-X), Soochow University, Suzhou, 215123, China.

Email: xinmingli@suda.edu.cn; xtian@suda.edu.cn.

Contents

1. Materials and methods

2-Chlorotrityl chloride resin, Fmoc-Asp (OtBu)-OH, Fmoc-Gly-OH, Fmoc-Phe-OH, and Fmoc-Arg(pbf)-OH were purchased from Shanghai GL Biochem (Shanghai, China). 8-Hydroxyquinoline-7-carboxylic acid, doxorubicin hydrochloride (DOX·HCl), and 3,3′,5,5′-tetramethylbenzidine (TMB) were obtained from Aladdin (Shanghai, China). $CuCl_2 \cdot 2H_2O$, $FeCl_3 \cdot 6H_2O$, and $MnCl_2$ were supplied by Sinopharm Chemical Reagent Co., Ltd. (Shanghai, China). Dulbecco's Modified Eagle Medium (DMEM) was purchased from Gibco (USA), and phosphate-buffered saline (PBS) was obtained from Bioind (ISR). Penicillin sodium and streptomycin were purchased from Dalian Meilun Biological Co., Ltd. (Dalian, China). Calf thymus DNA (ct-DNA) was obtained from Macklin (Shanghai, China). Tris(hydroxymethyl)aminomethane hydrochloride (Tris-HCl) was purchased from Thermo Fisher Scientific. pBR322 DNA was obtained from Takara Co., Ltd. (Suzhou, China). Ethidium bromide (EB) was provided by G-clone (Beijing, China). The reactive oxygen species (ROS) assay kit, Cell Counting Kit-8 (CCK-8), apoptosis assay kit, and live/dead cell staining reagents were supplied by Fcmacs Biotech Co., Ltd. (Nanjing, China). Hoechst 33342 was obtained from Beyotime Co., Ltd. (Shanghai, China). Human umbilical vein endothelial cells (HUVECs) and 4T1 murine breast cancer cells were purchased from Biobw Co., Ltd. (Beijing, China). The 808 nm laser (MDL-H-808 nm-5W-BH80521) was purchased from Changchun Laser Optoelectronics Technology Co., Ltd. (Changchun, China).

^1H NMR spectra were recorded on a Unity Inova 400 MHz spectrometer using DMSO-d_6 as the solvent. Matrix-assisted laser desorption/ionization time-of-flight mass spectrometry (MALDI-TOF MS) was performed on a Bruker Ultraflex-Treme mass spectrometer (Germany). Transmission electron microscopy (TEM) images were acquired using an HT7700 microscope (Japan). Fourier transform infrared (FTIR) spectra were obtained on a Nicolet 6700 spectrometer (Thermo Scientific, USA). UV-vis absorption spectra were recorded on a Shimadzu UV1900i spectrophotometer (Japan). Temperature changes during photothermal experiments were monitored using an infrared thermal camera (Fotric 225s, China). Confocal laser scanning

microscopy (CLSM) images for live/dead cell staining, ROS generation, and cellular uptake were acquired using a Zeiss confocal microscope (Germany).

2. Experimental Section

2.1 Peptide Synthesis

The peptide HQ-FFGGRGD was synthesized via standard solid-phase peptide synthesis (SPPS) using 2-chlorotrityl chloride resin as the solid support. Briefly, 0.6 g of resin was swollen in dry dichloromethane (DCM) under nitrogen bubbling for 30 min. After swelling, the resin was washed five times with dry N, N-dimethylformamide (DMF), followed by the addition of a DMF solution containing Fmoc-Asp (OtBu)-OH and N, N-diisopropylethylamine (DIEA). The coupling reaction was allowed to proceed for 1.5 h, after which the resin was washed four times with dry DMF. To cap any unreacted sites, the resin was treated with a blocking solution (DCM/MeOH/DIEA, 32:6:2, v/v/v) for 10 min and then thoroughly rinsed with dry DMF. The Fmoc protecting group was removed by treatment with 20% piperidine in DMF for 30 min, followed by four washes with DMF. The desired peptide sequence was elongated by sequential coupling of Fmoc-protected amino acids following standard Fmoc SPPS protocols. Upon completion of the synthesis, the peptide was cleaved from the resin using 95% trifluoroacetic acid (TFA). The crude product was purified by reversed-phase high-performance liquid chromatography (HPLC) using a gradient elution of H_2O/CH_3CN (from 80:20 to 20:80, v/v). The final yield of the purified HQ-FFGGRGD peptide was approximately 87%. The molecular structure was confirmed by ^1H NMR and mass spectrometry. ^1H NMR (400 MHz, DMSO) δ 9.30 (s, 1H), 8.56 (dd, J = 55.2, 44.9 Hz, 3H), 8.19 (dd, J = 31.7, 8.1 Hz, 2H), 8.12–7.88 (m, 4H), 7.83 (t, J = 8.3 Hz, 1H), 7.45 (dd, J = 8.2, 4.3 Hz, 1H), 7.37 (dd, J = 7.9, 4.3 Hz, 1H), 7.27 (t, J = 7.9 Hz, 2H), 7.24–7.17 (m, 3H), 7.11 (dt, J = 18.5, 9.1 Hz, 3H), 6.67 (s, 1H), 6.57 (d, J = 8.8 Hz, 1H), 4.67 (s, 1H), 4.48 (s, 1H), 4.29 (s, 1H), 4.14 (s, 1H), 3.79 (ddd, J = 43.9, 21.8, 8.7 Hz, 5H), 3.50 (d, J = 16.5 Hz, 1H), 3.20–2.97 (m, 4H), 2.85 (dd, J = 22.6, 9.3 Hz, 2H), 2.34 (d, J = 10.0 Hz, 1H), 2.06–1.95 (m, 1H), 1.85 (dd, J = 12.7, 7.0 Hz, 1H), 1.50 (t, J = 47.1 Hz, 4H). MS: calculated for $C_{44}H_{55}N_{11}O_{12}$ $[M]^+$ = 925.37; observed $[M+H]^+$ = 926.75, $[M+Na]^+$ = 948.72.

2.2 Preparation of HQD-Metal NPs and HQDCuD NPs

For the preparation of HQD-metal complexes, HQD was first dissolved in ultrapure water under ultrasonication to obtain a 5 mM stock solution. Subsequently, $CuCl_2 \cdot 2H_2O$, $MnCl_2$, or $FeCl_3 \cdot 6H_2O$ was added at molar ratios of HQD:Cu^{2+}/Mn^{2+} = 2:1 and HQD:Fe^{3+} = 3:1. The pH of the mixture was adjusted to 7.4 using 1 M NaOH solution, and the resulting solution was allowed to stand at room temperature (25 °C) to complete the coordination reaction. The product was then transferred into a dialysis membrane (MWCO = 1000 Da) and dialyzed against deionized water under dark conditions. The external dialysate was replaced every 4 h over a total of 48 h to thoroughly remove salt impurities. After dialysis, the solution was lyophilized under vacuum to obtain the purified HQD-metal complex. For self-assembly, the lyophilized product was re-dissolved in deionized water (pH 7.4) to yield a clear, transparent solution with a concentration of 0.2 wt%.

To prepare DOX-loaded nanoparticles (HQDCuD), an equal mass of DOX was added to the HQD solution under constant stirring at 500 rpm, followed immediately by the addition of $CuCl_2 \cdot 2H_2O$ solution. The mixture was stirred for 12 h, then dialyzed against deionized water using a dialysis membrane (MWCO = 1000 Da) for 24 h. The resulting HQDCuD nanoparticles were collected for subsequent characterization.

2.3 Transmission Electron Microscopy (TEM)

The morphology of the self-assembled nanostructures was observed using a Hitachi HT7700 transmission electron microscope. Briefly, 4 μL of each sample was deposited onto a carbon-coated copper grid, negatively stained with 2.0% (w/v) phosphotungstic acid for 8–10 min, and air-dried prior to imaging.

2.4 Particle Size and Zeta Potential Measurement

Hydrodynamic diameter and zeta potential of HQD-metal and HQDCuD nanoparticles were measured by dynamic light scattering (DLS) using a Zetasizer instrument. Briefly, 200 μL of the nanoparticle solution was injected into a cuvette and analyzed at room temperature.

2.5 Fourier Transform Infrared (FTIR) Spectroscopy

FTIR spectra were recorded on a PerkinElmer spectrophotometer. Samples were prepared in deuterated water (D_2O) and loaded into potassium bromide (KBr) cuvettes. Spectra were collected over the range of 4000–600 cm^{-1} with 64 scans per measurement.

2.6 Circular Dichroism (CD) Spectroscopy

CD spectra were recorded on a Jasco J-810 spectrophotometer. Samples (25 μL) were placed in a quartz cuvette with a 1 mm path length and scanned from 185 to 300 nm under a nitrogen atmosphere.

2.7 DNA Binding Studies by UV-Vis Absorption Titration

Calf thymus DNA (ct-DNA) stock solution was prepared in Tris-HCl buffer (10 mM, pH 7.4), and its concentration was determined spectrophotometrically at 260 nm using the molar extinction coefficient ε = 6600 $M^{-1} \cdot cm^{-1}$. UV-vis titration experiments were performed by maintaining a fixed concentration of HQD-metal complexes (50 μM) while gradually adding increasing amounts of ct-DNA (10–100 μM). After each addition, the solution was allowed to equilibrate for 40 min at room temperature before recording the spectrum. A reference cuvette containing the same concentration of ct-DNA was used to eliminate the intrinsic absorbance of DNA. Spectral changes were monitored to evaluate DNA binding behavior.

2.8 DNA Binding Studies by Competitive Fluorescence Titration

Competitive fluorescence titration assays were conducted to evaluate the ability of HQD-metal complexes to displace DNA-bound fluorophores. Briefly, ct-DNA (100 μM) in Tris-HCl buffer (10 mM, pH 7.4) was pre-incubated with either ethidium bromide (EB, 20 μM) or Hoechst 33342 (20 μM) for 30 min to form fluorescent DNA adducts. Aliquots of HQD-metal complexes (0–100 μM) were then added incrementally, and the mixtures were equilibrated at room temperature. Fluorescence spectra were recorded at excitation wavelengths of 510 nm (for EB) and 350 nm (for Hoechst 33342). The decrease in fluorescence intensity was analyzed using the modified Stern–Volmer equation, and binding affinities were quantified by plotting F_0/F against complex concentration, where F_0 and F represent fluorescence intensities in the absence and presence of the complex, respectively.

2.9 Agarose Gel Electrophoresis for DNA Cleavage Assay

The DNA cleavage activity of HQD-metal complexes was assessed using supercoiled pBR322 plasmid DNA. Electrophoresis was carried out in TBE buffer (prepared from a 10× stock containing 21.56 g Tris, 11.01 g boric acid, and 1.41 g EDTA per liter, pH 8.0). For each cleavage reaction, pBR322 DNA (0.5 g/L, 0.5 μL) was mixed with H_2O_2 (0.05 mM, 3 μL) and the respective metal complex (0.5 mM) in Tris-HCl buffer to a final volume of 15 μL. The mixture was incubated at 37 °C for 30 min. After incubation, 10 μL of the reaction mixture was combined

with 1 μL of loading buffer and loaded onto a 0.8% agarose gel containing 0.01% GoldView nucleic acid stain. Electrophoresis was performed in 1× TBE buffer at 80 V for 80 min. DNA bands were visualized under UV illumination, and the extent of plasmid cleavage was analyzed based on the conversion of supercoiled (Form I) to nicked circular (Form II) and linear (Form III) DNA.

2.10 Photothermal Performance Evaluation

The photothermal properties of the HQD-metal nanoparticles were evaluated under 808 nm laser irradiation. Briefly, 300 μL of each sample solution was transferred into a 96-well plate and irradiated with an NIR laser at designated power densities for a predetermined duration. Real-time temperature changes were monitored using an infrared thermal camera (Fotric 225s, China). Temperature profiles were recorded during both the heating and natural cooling phases.

The photothermal conversion efficiency (η) was calculated according to the following equation:

$$\eta = \frac{hS\left(T_{max} - T_{surr}\right) - Q_s}{I\left(1 - 10^{-A_\lambda}\right)}$$

where T_{max} is the equilibrium temperature after laser irradiation, T_{surr} is the ambient temperature, Qs represents the heat absorbed by the solvent (water) under irradiation, I is the laser power density (W cm^{-2}), and A_λ is the absorbance of the nanoparticle solution at 808 nm. The heat transfer coefficient hS was determined from the cooling profile using the following relationship:

$$hS = \frac{mC_{H2O}}{\tau_s}$$

with m is the mass of the solution (g), C_{H2O} is the specific heat capacity of water (4.2 J /g °C), and τs is the system time constant. The value of τs was obtained by fitting the cooling curve to the linear equation:

$$t = -\tau_s In\theta = -\tau_s In\left(\frac{T - T_{surr}}{T_{max} - T_{surr}}\right)$$

2.11 Evaluation of Peroxidase-Like Catalytic Activity

The peroxidase-like activity of HQD-metal complexes was evaluated by monitoring the catalytic oxidation of 3,3,5,5-tetramethylbenzidine (TMB) in the presence of H_2O_2. In a typical assay, TMB (0.2 mM) and H_2O_2 (5 mM) were mixed in PBS buffer (10 mM, pH 7.4) to form the reaction matrix, followed by brief vortexing. The catalytic reaction was initiated by adding the

complex solution, and the formation of oxidized TMB (oxTMB) was monitored by measuring the absorbance at 650 nm using a UV-vis spectrophotometer. The catalytic activity was evaluated under varying conditions, including different temperatures (25, 37, and 60 °C) and pH values (5.0, 6.5, and 7.4). Reaction kinetics were assessed based on the time-dependent absorbance changes at 650 nm to compare catalytic efficiencies across experimental groups.

2.12 Identification of Reactive Oxygen Species Involved in TMB Oxidation

To identify the reactive oxygen species (ROS) responsible for TMB oxidation, radical scavenging experiments were performed. Briefly, superoxide dismutase (SOD, 40 μL, 3×10^{-3} M in PBS) or tert-butanol (TBA, 60 μL, 3 M in ultrapure water) was added to the catalytic system containing TMB (0.2 mM), H_2O_2 (5.0 mM), and HQDCu (25 μM) in PBS buffer. The formation of oxTMB was monitored by measuring the absorbance at 650 nm over time using a UV-vis spectrophotometer (UV-1900i). The decrease in absorbance in the presence of scavengers indicated the involvement of specific ROS species.

2.13 GPx-Like Catalytic Activity Assay

The glutathione peroxidase (GPx)-like activity of HQD-metal complexes was assessed by monitoring the time-dependent oxidation of glutathione (GSH). HQDCu nanoparticles at various concentrations (0, 0.05, 0.1, 0.15, and 0.2 mM) were incubated with GSH (1 mM) at 25, 37, or 60 °C. At predetermined time intervals, aliquots of the reaction mixture were withdrawn and reacted with DTNB (10 mM) for 5 min. The absorbance at 412 nm was then measured to quantify the remaining GSH content. The decrease in absorbance reflected the extent of GSH oxidation.

2.14 In Vitro DOX Release Study

The release profile of doxorubicin (DOX) from HQDCuD nanoparticles was evaluated using a dialysis method. Briefly, 1 mL of HQDCuD dispersion was placed into a dialysis bag (MWCO: 1000 Da) and immersed in 20 mL of PBS at different pH values (7.4, 6.5, and 5.0). The samples were incubated at 37 °C with gentle shaking (100 rpm). At designated time intervals, 4 mL of the external medium was withdrawn for analysis and replaced with an equal volume of fresh pre-warmed PBS. The concentration of released DOX was quantified by measuring the absorbance at 480 nm using a UV-vis spectrophotometer.

2.15 Cellular Uptake Study

Cellular uptake of HQDCuD nanoparticles was evaluated in 4T1 cells using confocal laser scanning microscopy (CLSM). Cells were seeded in confocal dishes at a density of 1.0×10^5 cells per well and allowed to adhere overnight. The medium was then replaced with fresh DMEM containing free DOX (4 μg mL^{-1}) or HQDCuD (80 μg mL^{-1}). After incubation for 3 or 6 h, cells were stained with Hoechst 33342 (10 μM) for 15 min, followed by three washes with PBS. Fluorescence images were acquired using a CLSM (Hoechst: Ex = 350 nm; DOX: Ex = 480 nm).

2.16 Cytotoxicity Assay

The cytotoxicity of various formulations toward 4T1 and HUVEC cells was assessed using the Cell Counting Kit-8 (CCK-8) assay. Cells were seeded in 96-well plates at a density of 8×10^3 cells per well in 100 μL of DMEM and allowed to adhere overnight. The medium was then replaced with fresh medium containing the indicated concentrations of each formulation. For photothermal treatment groups, cells were irradiated with an 808 nm laser (1.0 W cm^{-2}) for 8 min. Untreated cells served as the control group. After 24 h of incubation, the medium was replaced with 100 μL of CCK-8 working solution (10% in DMEM) and incubated for an additional 30 min. Absorbance at 450 nm was measured using a microplate reader, and cell viability was calculated relative to the control group.

2.17 Live/Dead Cell Staining

Live/dead staining was performed to visually assess the cytotoxicity of various treatments. 4T1 cells were seeded in confocal dishes at a density of 1.5×10^5 cells per well and allowed to adhere overnight. Cells were then treated with the indicated formulations for 24 h, followed by NIR irradiation (808 nm, 1.0 W cm^{-2}, 8 min) where applicable. After treatment, cells were washed three times with PBS and incubated with a staining solution containing Calcein-AM (1 μM) and propidium iodide (PI, 4 μM) at 37 °C for 20 min. Fluorescence images were acquired using a CLSM (Calcein-AM: Ex = 490 nm; PI: Ex = 488 nm).

2.18 Cell Apoptosis Assay

Apoptosis was quantitatively evaluated using an Annexin V-FITC/PI apoptosis detection kit. 4T1 cells were seeded in 6-well plates at a density of 1.5×10^5 cells per well and allowed to adhere overnight. Cells were then treated with the indicated formulations for 24 h, followed by NIR irradiation (808 nm, 1.0 W cm^{-2}, 8 min) where applicable. After treatment, cells were harvested by trypsinization, centrifuged at 1000 rpm for 5 min, washed three times with cold PBS, and

resuspended in 500 μL of Annexin V binding buffer. Subsequently, 10 μL of Annexin V-FITC and 5 μL of PI were added, and the samples were incubated at 37 ℃ for 15 min in the dark. Apoptotic cells were quantified using flow cytometry, and data were analyzed with FlowJo software.

2.19 Intracellular ROS Generation

Intracellular reactive oxygen species (ROS) levels were assessed using the DCFH-DA probe. 4T1 cells were seeded in plates at a density of 1.2×10^5 cells per well and allowed to adhere for 12 h. Cells were then treated with each formulation (50 μg mL^{-1}) for 6 h. After treatment, the medium was removed, and cells were washed with PBS, followed by incubation with fresh medium containing 10 μM DCFH-DA for 30 min. The probe solution was then discarded, and cells were washed with PBS. Intracellular ROS-associated fluorescence was visualized using an Olympus fluorescence imaging system (Ex = 480 nm). For quantitative analysis, parallel samples were analyzed by flow cytometry.

2.20 Intracellular GSH Depletion

Intracellular glutathione (GSH) levels were evaluated using ThiolTrace™ Violet staining. 4T1 cells were seeded in confocal dishes at a density of 1.2×10^5 cells per well and incubated overnight. Cells were then treated with each formulation (50 μg mL^{-1}) for 6 h, followed by NIR irradiation (808 nm, 1.0 W cm^{-2}, 8 min) where applicable. After treatment, cells were incubated with ThiolTrace™ Violet (20 μM) for 30 min, washed with PBS, and imaged using an Olympus fluorescence imaging system (Ex = 405 nm). For quantitative assessment of GSH depletion, parallel samples were analyzed by flow cytometry.

3. Synthesis and Structural Characterization of the HQ-FFGGRGD Conjugate

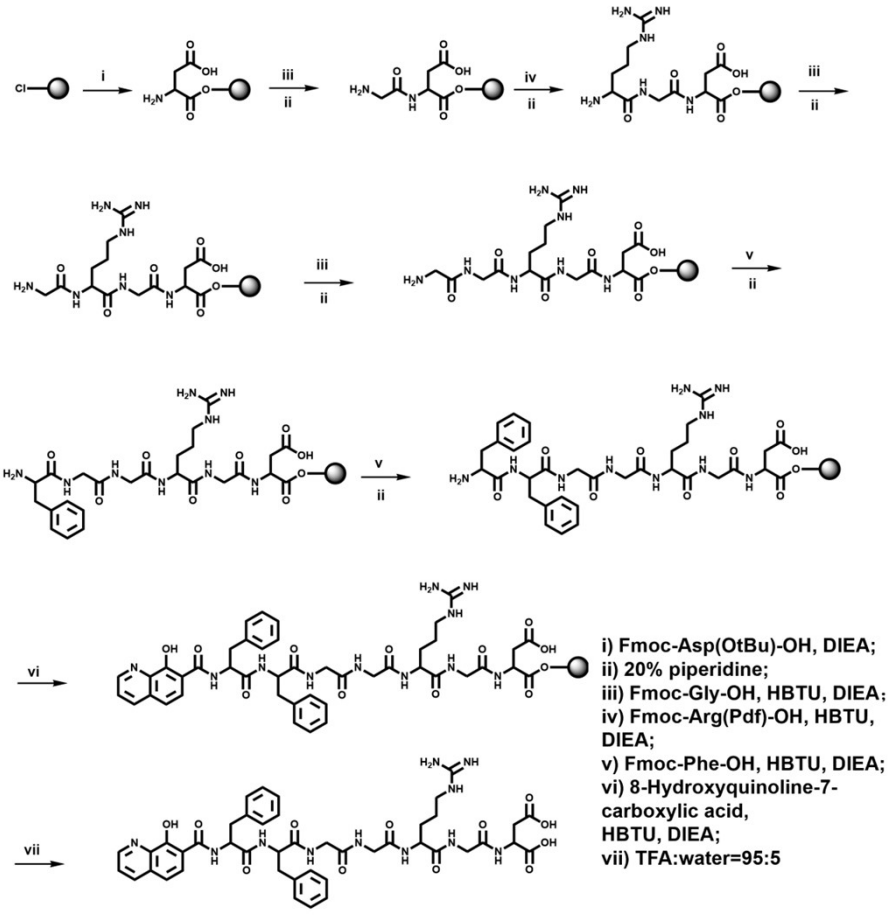

Fig. S1 Synthetic route for the preparation of HQD via solid-phase peptide synthesi s.

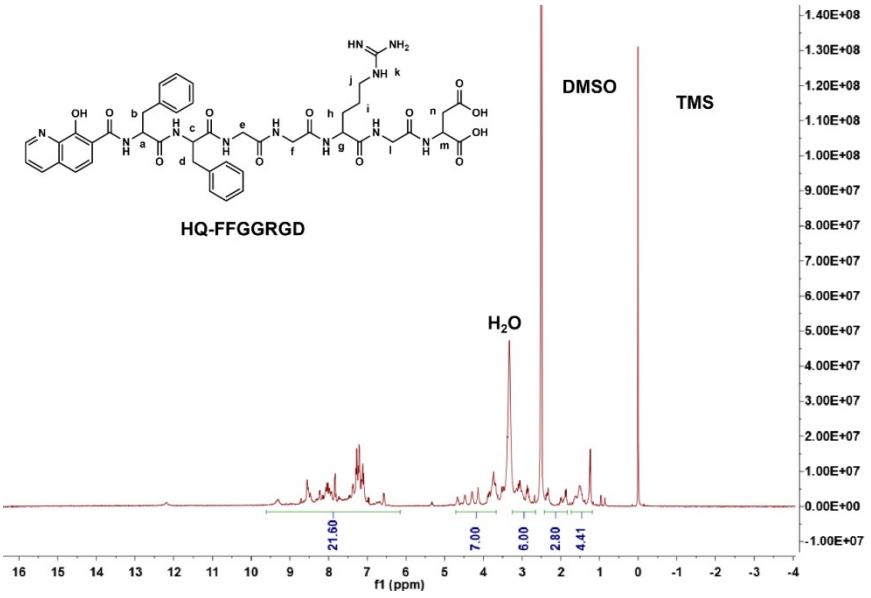

Fig. S2 ^{1}H NMR of HQD in DMSO-*d6*.

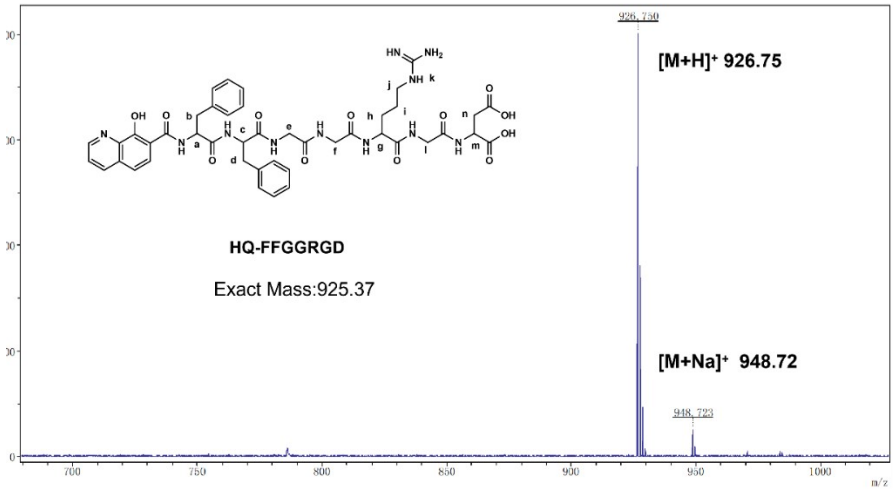

Fig. S3 MALDI-TOF MS of HQD.

4. Morphologies of Self-Assembled HQD Nanostructures in Aqueous Solutions

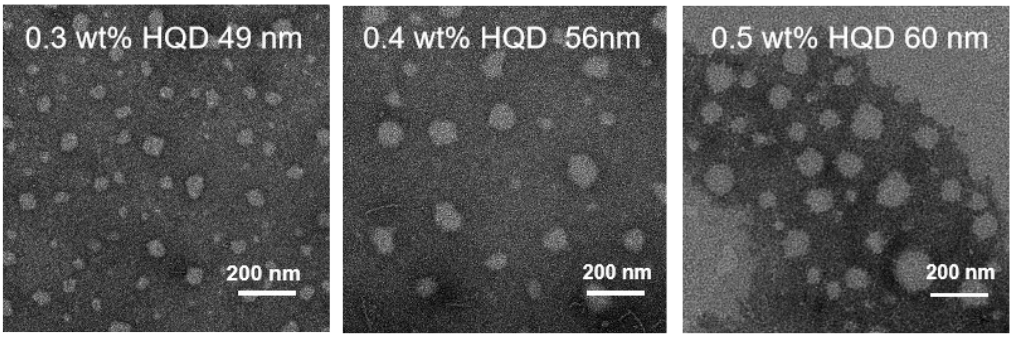

Fig. S4 TEM characterization of HQD nanostructures at varied concentrations (0.3, 0.4 and 0.5 wt%).

5. Determination of the Binding Stoichiometry between HQD and Metal Ions

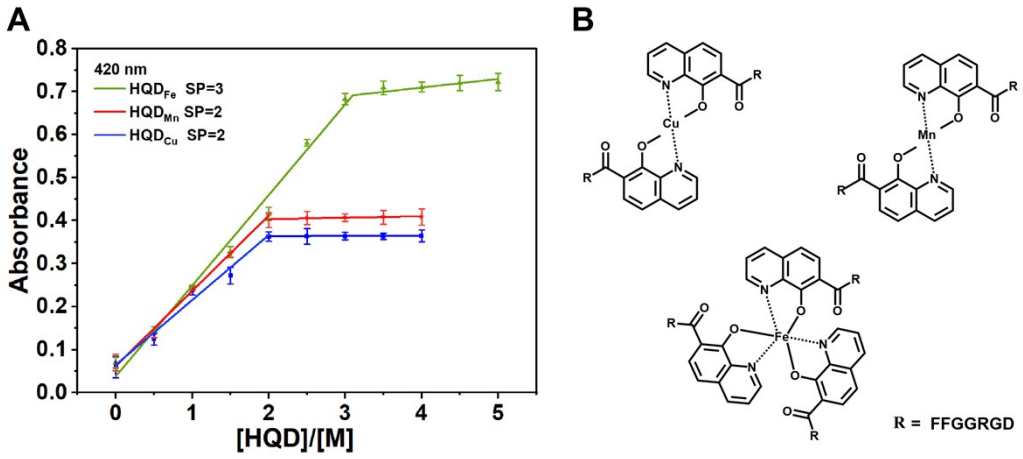

Fig. S5 (A) The Molar ratio plots for the determination of coordination stoichiometry bet ween HQD and metal ions. The concentrations of $CuCl_2 \cdot 2H_2O$, $FeCl_3 \cdot 6H_2O$, and $MnCl_2$ w ere maintained at 0.5 mM. (B) Schematic diagram of the coordination geometries for HQ D_{Cu}, HQD_{Mn}, and HQD_{Fe}. The stoichiometric ratios are HQD:Cu^{2+}/Mn^{2+} = 2:1 and HQD:F e^{3+} = 3:1.

6. Time-Dependent Particle Size Stability of HQD and HQD-Metal Nanoparticles

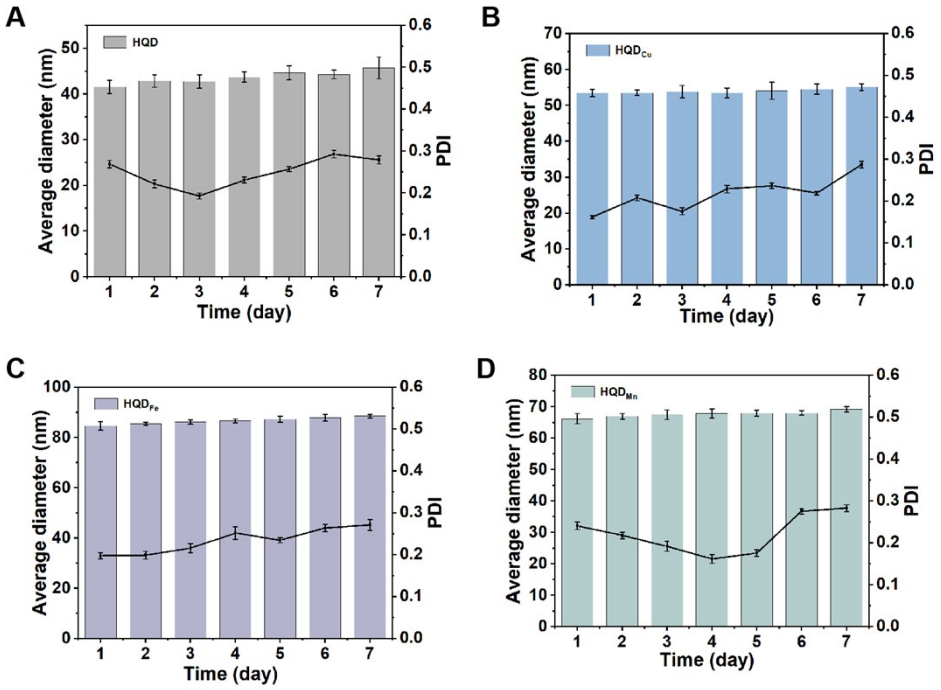

Fig. S6 Hydrodynamic size and size distribution of HQD and HQD-metal nanoparticles over 7 days, as determined by DLS in aqueous solution.

7. Assessment of DNA Binding Modes and Affinities of HQDFe and HQDMn via Competitive Fluorescence Titration

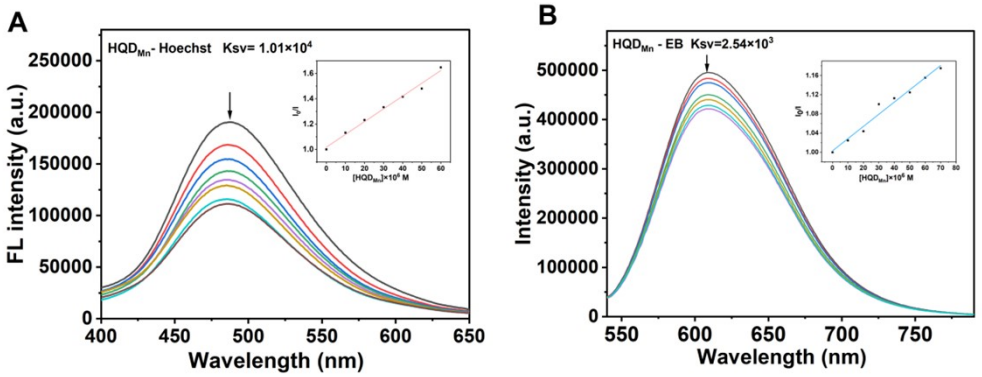

Fig. S7 Competitive fluorescence titration assays of HQD_{Mn} with DNA-bound fluorophores. (A) Fluorescence spectra of Hoechst 33342 bound to ct-DNA upon incremental addition of HQD_{Mn}. (B) Fluorescence spectra of EB bound to ct-DNA upon incremental addition of HQD_{Mn}.

Conditions: [DNA] = 1.0 × 10^{-4} M, [Hoechst] = [EB] = 2.0 × 10^{-5} M. Insets show the Stern–Volmer plots and the corresponding quenching constants (K_{sv}).

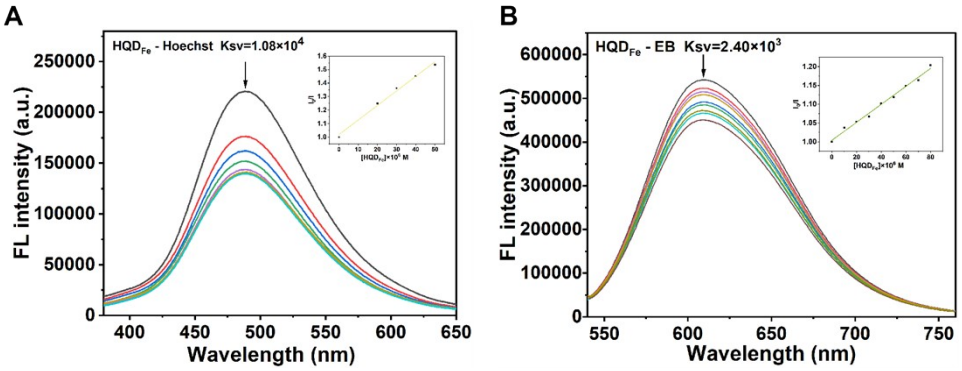

Fig. S8 Competitive fluorescence titration assays of HQD_{Fe} with DNA-bound Hoechst and EB. (A) Fluorescence spectra of Hoechst–DNA complex upon addition of HQDFe. (B) Fluorescence spectra of EB–DNA complex upon addition of HQD_{Fe}. [DNA] = 1.0 × 10^{-4} M, [Hoechst] = [EB] = 2.0 × 10^{-5} M. Insets: Stern–Volmer plots with calculated K_{sv} values for HQD_{Fe}.

8. Evaluation of DNA Binding by the HQ Ligand via UV-Vis Absorption and Fluorescence Titration

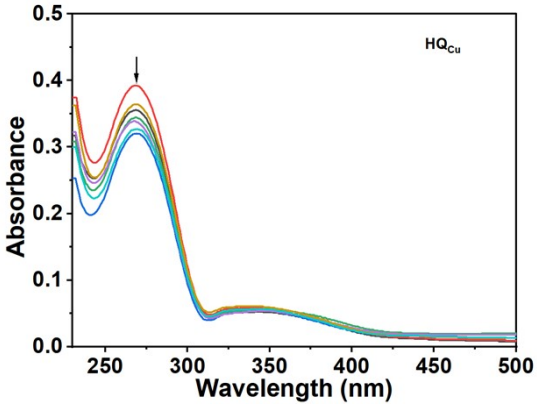

Fig. S9 UV-vis absorption spectra of HQ (50 μM) incubated with increasing amounts of DNA (0-70 μM).

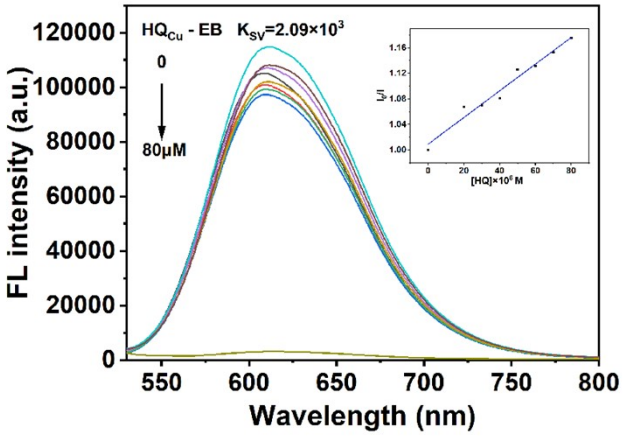

Fig. S10 Competitive binding assay of HQ with the EB–DNA complex. Fluorescence spectra show the quenching of EB (2.0×10^{-5} M) bound to ct-DNA (1.0×10^{-4} M) upon titration with HQ. The inset presents the Stern-Volmer plot used to calculate the quenching constant (K_{sv}).

9. Near-Infrared Absorption Spectra of HQD and HQD- Metal Complexes

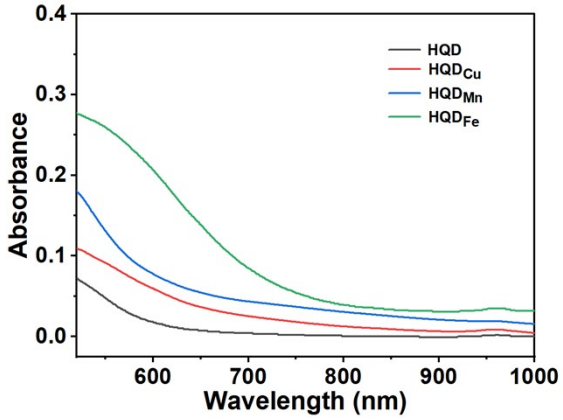

Fig. S11 Absorption spectra of HQD and HQD-metal complex solutions (50 μg/mL) in the near-infrared region (650–900 nm).

10. Concentration-Dependent Photothermal Performance of HQD_{Cu} and HQD_{Mn}

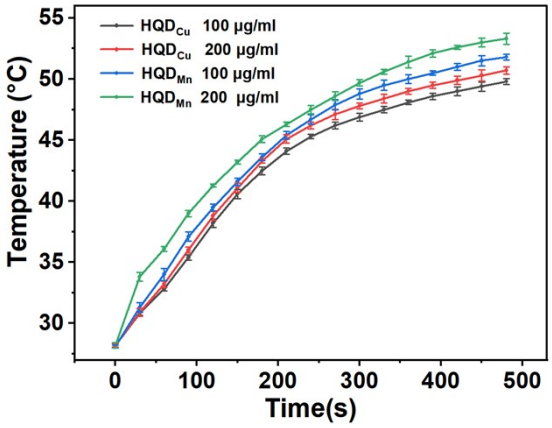

Fig. S12 Concentration-dependent photothermal performance of HQD_{Cu} and HQD_{Mn}. Temperature elevation of nanoparticle solutions at concentrations of 100 and 200 μg mL^{-1} was monitored over 8 min of 808 nm laser irradiation (1.0 W cm^{-2}).

11.Photothermal Conversion Efficiency of HQD_{Mn} and HQD_{Cu}.

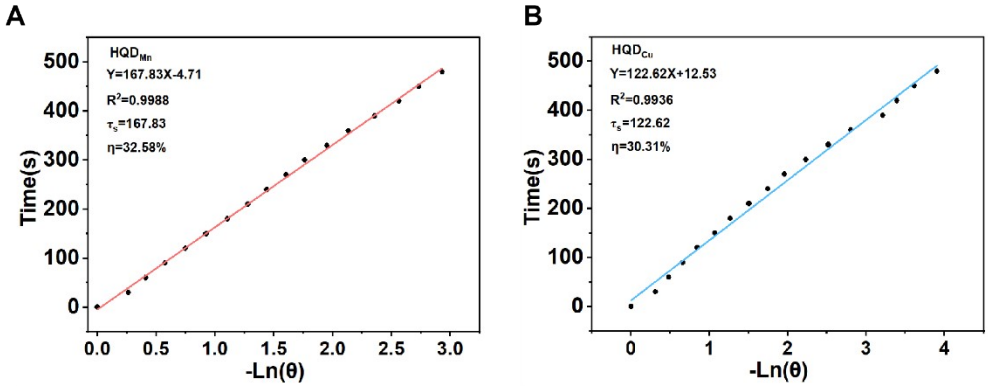

Fig. S13 Linear fitting of the cooling period versus -lnθ for the determination of the photothermal conversion efficiency (η) of (A) HQD_{Mn} and (B) HQD_{Cu}.

12. Temperature-Dependent GPx-Like Activity of HQD_{Cu}

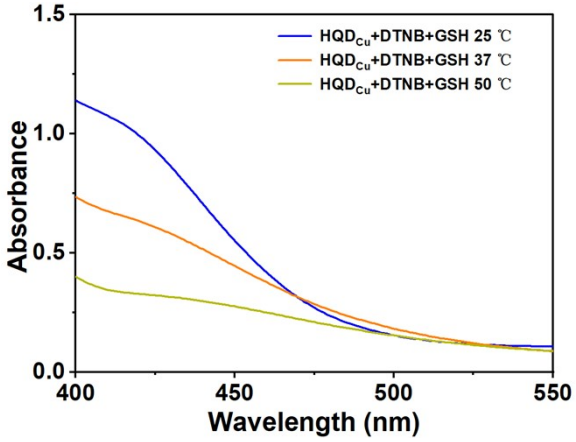

Fig. S14 UV-vis absorption spectra showing the HQD_{Cu}-catalyzed oxidation of GSH at various temperatures (25, 37, and 50 °C).

13. Concentration-Dependent DNA Cleavage Activity of HQDCu Nanoparticles

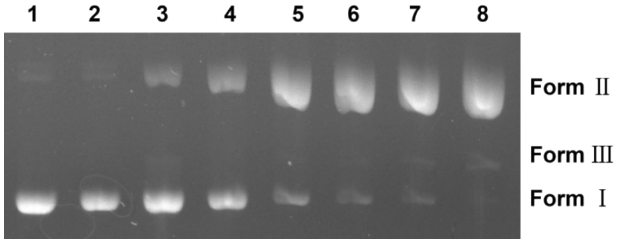

Fig. S15 Agarose gel electrophoresis analysis of pBR322 DNA cleavage by HQD_{Cu} at varying concentrations. Reaction conditions: [H_2O_2] = 0.1 mM, pH 7.4, 37 °C, 1 h incubation. Lane 1: DNA alone; lanes 2–8: DNA + H_2O_2 + HQD_{Cu} at 0.05, 0.08, 0.1, 0.2, 0.3, 0.4, and 0.5 mM, respectively.

14. Drug-Loading Properties of Anticancer Drug of DOX

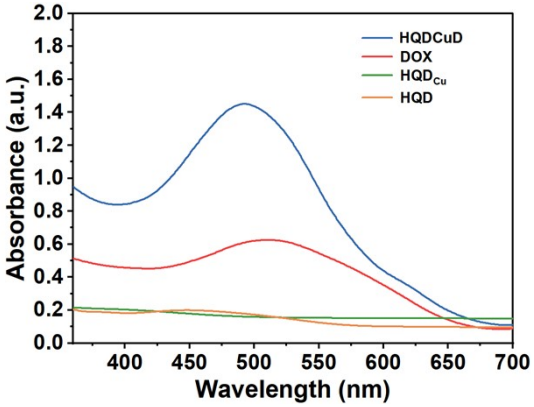

Fig. S16 UV-vis absorption spectra confirming the successful loading of DOX into HQD_{Cu} nanoparticles. Spectra of free DOX, HQD_{Cu}, and HQDCuD are shown for comparison.

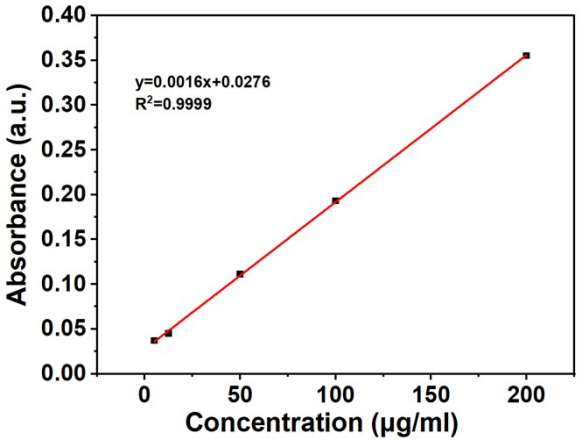

Fig. S17 Standard curve for doxorubicin (DOX) quantification. Absorbance at 480 nm was plotted against DOX concentration to establish the linear regression equation.

15. The Particle Size and Zata Potential of HQDCuD NPs.

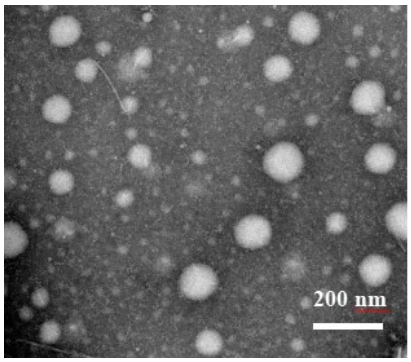

Fig. S18 TEM characterization of HQDCuD at the condition of 0.2 wt% and pH 7.4.

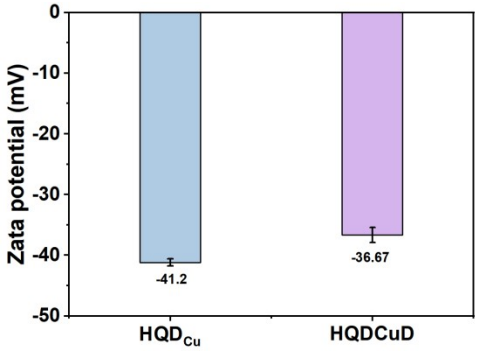

Fig. S19 Zeta potentials of HQD_{Cu} and HQDCuD nanoparticles measured at 0.2 wt% and pH 7.4.

16. Cellular Uptake of Free DOX and HQDCuD Nanoparticles

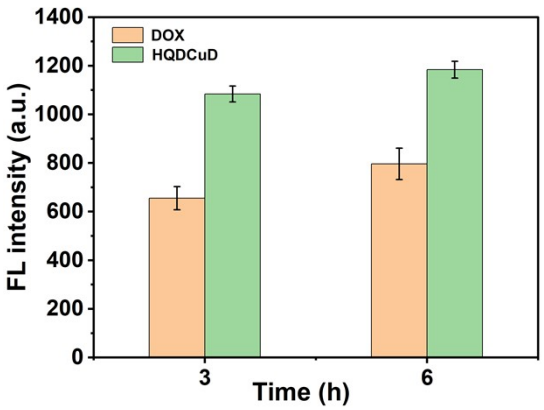

Fig. S20 Flow cytometry analysis of 4T1 cells after treatment with free DOX or HQDCuD nanoparticles for 3 and 6 h.

17. In Vitro Cytotoxicity of HQD-Metal Nanoparticles Against Human Umbilical Vein Endothelial Cells (HUVECs)

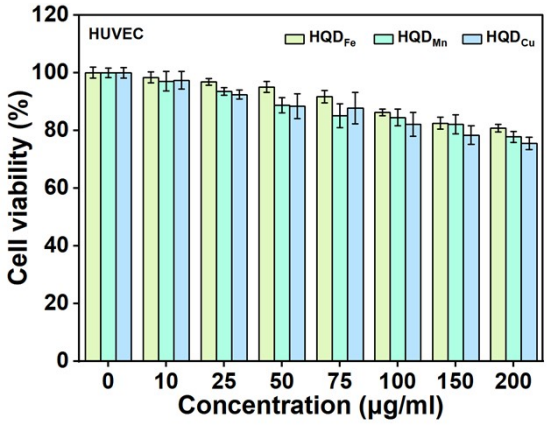

Fig. S21 Cytotoxicity evaluation of HQD-metal nanoparticles in normal human cells. HUVECs were incubated with increasing concentrations (10, 25, 50, 75, 100, 150, and 200 μg mL^{-1}) of HQD_{Cu}, HQD_{Fe}, or HQD_{Mn} nanoparticles for 24 h, and cell viability was determined by CCK-8 assay.

18. Cytotoxic Dose-Response Curves and IC_{50} Values of HQD-Metal Complexes Against 4T1 Cells.

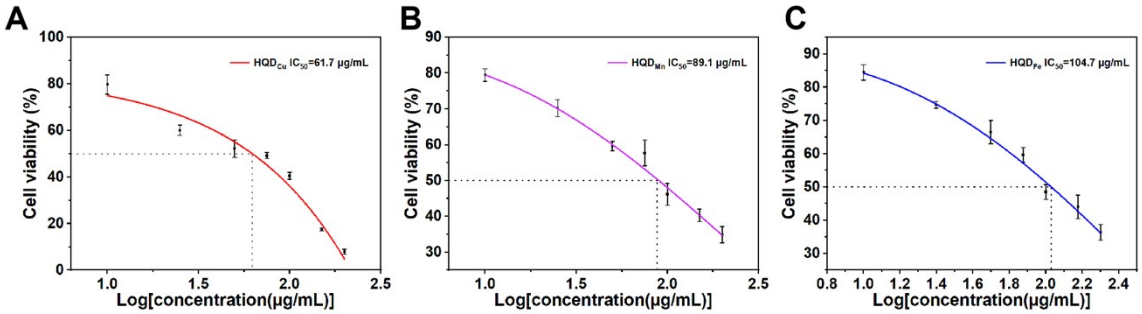

Fig S22 Cytotoxic dose-response curves and IC_{50} values of HQD_{Cu}(A), HQD_{Mn}(B), and HQD_{Fe}(C) groups based on the cell viability data. $IC_{50}(HQD_{Cu})$ = 61.7 μg/mL, $IC_{50}(HQD_{Mn})$ = 89.1 μg/mL, $IC_{50}(HQD_{Fe})$ = 104.7 μg/mL.